MINERALOGICAL MAGAZINE, MARCH 1986, VOL. 50, PP. 3–15

Ion microprobe determination of rare earth elements in accessory minerals

S. J. B. REED

Department of Earth Sciences, University of Cambridge, Cambridge CB3 0EZ

ABSTRACT. The application of ion microprobe analysis to *REE* determination is discussed, with special reference to *REE*-bearing accessory minerals (e.g. allanite, monazite, apatite, xenotime, sphene). The main analytical problems are shown to be (*a*) interferences in the mass spectrum caused by molecular ions, and (*b*) matrix effects, i.e. variations in ion yield with sample composition. Interference suppression using either high mass resolution or secondary-ion energy discrimination is fairly effective, but entails a significant sacrifice in peak intensity. In the absence of a viable model for predicting matrix effects, it is proposed that empirical standardization should be used. Often better absolute accuracy can be obtained by combining ion microprobe and electron microprobe data for *REE* present in sufficiently high concentrations. Detection limits for *REE* are in the part per million region at present, with spatial resolution typically around 10 μm, but there is considerable scope for improvement. Better standards and improved understanding of matrix effects should also lead to greater accuracy in quantitative analysis.

KEYWORDS: ion microprobe, rare earth elements, allanite, apatite, sphene, chevkinite.

THE geochemistry of the rare earth elements (*REE*) is a topic of considerable interest (see Henderson, 1984, for a recent review). The similarity of the chemical properties of the lanthanides (La–Lu) results from the outermost electron shell being completely filled. However, with increasing atomic number the radius of the trivalent ions, in which form these elements normally exist, decreases (the 'lanthanide contraction'). The ionic radius is the main factor determining the ability of a crystalline phase to accommodate *REE* and controls their distribution, although environment and availability of *REE* can also have a considerable influence.

Common rock-forming silicates generally have low *REE* concentrations (mostly below 10 ppm), owing to the incompatibility of the relatively large ions of the *REE* with the crystal structures concerned. The bulk *REE* content of igneous rocks, however, is commonly in the region of several hundred ppm, with accessory phases acting as hosts for these elements. These accessory minerals have an important influence on the behaviour of *REE* in igneous and metamorphic rock formation.

Three categories of *REE* host-minerals exist: first, those in which *REE* play an essential and exclusive part in the crystal chemistry (the *REE* phosphate monazite is an example). Second, *REE*-rich variants of usually *REE*-poor phases, in which there is major substitution by *REE* for other elements (e.g. allanite, the *REE*-rich version of epidote). Finally, there are minerals in which *REE* play a non-essential role as minor substituents but which are significant as *REE* hosts (e.g. apatite). This paper is concerned with the application of ion microprobe analysis to *REE* determination in all three types of accessory mineral.

The analytical problem has two somewhat distinct aspects: first, the determination of the *REE* distribution pattern, for which only relative *REE* concentrations are needed, and secondly obtaining absolute concentrations in order to arrive at a complete analysis of the mineral concerned. As will be shown below, the ion microprobe is better suited to the former task than the latter, but in many cases both needs can be satisfied adequately by combining electron and ion microprobe data.

It is usual to plot *REE* distribution patterns with concentrations normalized relative to 'chondritic abundances', considered to be representative of undifferentiated mantle material (see Table I). The 30:1 range in these abundances means that some *REE* are easier to determine accurately than others.

TABLE I. *Chondritic abundances of REE (ppm) (after Haskin* et al., *1968)*

La	0.33	Tb	0.047
Ce	0.88	Dy	0.32
Pr	0.112	Ho	0.070
Nd	0.60	Er	0.20
Sm	0.18	Tm	0.030
Eu	0.07	Yb	0.20
Gd	0.25	Lu	0.034

Where particular elements are determinable only with low accuracy, or not at all, there is a case for omitting them and relying on the others to delineate the shape of the distribution.

Though chondrite-normalized plots vary widely in shape, they are usually *smooth* (apart from Eu—see below). This permits interpolation for *REE* which cannot be determined accurately; further, it allows an internal check, inasmuch as lack of smoothness is likely to be attributable to analytical error. Eu commonly behaves anomalously because of its divalent tendencies, the Eu concentration in accessory minerals often being lower than the 'expected' value. In highly oxidizing sedimentary environments a Ce anomaly also sometimes occurs.

Hitherto, most *REE* analyses have been obtained by bulk methods (e.g. neutron activation) which require mineral separation as a preliminary to the analysis of individual mineral components of a rock. Whilst this is a reasonable proposition for rock-forming silicates, it is often impracticable for accessory minerals, which are sparsely distributed and usually of small grain-size. In such a situation a microbeam technique is advantageous, the most widely available being electron microprobe analysis, which has high spatial resolution (around 1 μm) and is non-destructive. However, this technique has rather high detection limits, owing to the continuum background in the X-ray spectrum. Furthermore, the *REE* spectrum is crowded with lines, resulting in overlaps and difficulty in establishing the true background. With wavelength-dispersive spectrometers, the practical detection limit for *REE* is generally no better than 200 ppm.

The continuum background is much less if protons rather than electrons are used to bombard the specimen, as in 'PIXE' (proton-induced X-ray emission), and in principle much lower detection limits are achievable, with a spatial resolution of a few μm. However, the *REE* are not ideal candidates for this technique—their *L* spectra lie in a region where the continuum emitted by secondary electrons enhances the background substantially, and the *K* lines, while free of this effect, are very weak.

The ion microprobe offers much lower detection limits for *REE* than the electron microprobe, with spatial resolution of several μm. Though the technique is not strictly non-destructive, the sample consumption of around 1 ng is negligible for most purposes. In the ion probe the specimen is bombarded with a focused beam of primary ions, causing the ejection of secondary ions. The secondary-ion mass spectrum is almost free of background, and if it were not for interferences caused by molecular ions, detection limits as low as a few parts per billion would be attainable, though practical detection limits for *REE* are nearer 1 ppm at present.

Quantitative analysis is hindered by the lack of a viable model from which to derive matrix corrections and, on the other hand, shortage of good standards. It may sometimes be appropriate to combine ion microprobe data for relative *REE* concentrations with electron microprobe data (of greater absolute accuracy), where the concentrations at least of the more abundant *REE* are high enough.

Experimental

The instrument used for the ion probe measurements reported here was a modified AEI IM-20 (Banner and Stimpson, 1974), with power supplies of improved stability, turbo-molecular vacuum pumps, and a new secondary-ion extraction assembly. In order to control the magnetic field of the mass spectrometer a computer-based system was developed, employing a 19-bit digital-to-analogue converter and a Hall probe as field monitor (Long *et al.*, 1980). The magnet coils (re-wound for low voltage operation) are driven by dual 500-watt audio amplifiers. The field is controlled by a computer, with software incorporating a mass calibration function enabling any mass from 1 to 256 to be selected, and a variety of operating routines.

The primary beam column consists of a duoplasmatron ion source, a magnetic sector mass filter and two electrostatic lenses. For the present measurements, $^{16}O^-$ primary ions were used, with an energy of 30 keV relative to the specimen. The mass filter serves to eliminate other, possibly undesirable, species such as OH^-. With insulating specimens, charge build-up is avoided by using negative primary ions, owing to the compensating effect of secondary electron emission. The diameter of the beam as used here was 15–20 μm and the current 15–20 nA.

A potential of +10 kV applied to the specimen accelerates positive secondary ions towards the mass spectrometer. The extraction system consists of an extraction cone, an electrostatic einzel lens, and a quadrupole lens producing a line focus on the horizontal entrance slit of the mass spectrometer. The quadrupole was designed by Degreve *et al.* (1979), and incorporates horizontal and vertical deflection plates. It is desirable to minimize changes in the electrostatic field distribution in front of the specimen on moving from one area to another. A fixed plate at the same potential as, and just in front of, the specimen helps to achieve this objective. Any residual effect of moving the specimen can be corrected by fine adjustment of extraction system potentials (principally those controlling vertical deflection).

The mass spectrum is recorded by sweeping the field of the mass spectrometer magnet and recording the secondary-ion intensity. The ions are detected by an electron multiplier and intensities are recorded by ion counting, using either a ratemeter for analogue output, or a digital scaler. Complete *REE* spectra may be obtained by sweeping from mass 139 to 192 (which includes all the significant monatomic and oxide peaks) and recording the ratemeter output. This approach is satisfactory when the peak intensities are reasonably high, but is unsuitable for use at high mass resolution. With computer-controlled

step-scanning, greater counting efficiency can be obtained by omitting peaks not required for analytical purposes. Also, at high mass resolution the region scanned can be limited to the immediate vicinity of the peaks.

Interferences—general

At low mass resolution, ions of the same nominal mass, including molecular ions and isobars of different elements, are indistinguishable (isobaric interferences amongst the *REE* are discussed in the following section). The atoms of which molecular ions are composed may originate from the specimen itself, the bombarding beam, or contaminants. Different species with the same mass number can in principle be distinguished by virtue of their differing mass defect, this being the amount by which the actual mass differs from the mass number, usually expressed in thousandths of a mass unit, or mmu. However, the mass differences involved are small, and in order to obtain the necessary mass resolution, narrow slits must be used in the mass spectrometer, with a serious loss of transmission. In the case of the AEI IM-20, a resolution of 3000 entails an intensity reduction of a factor of 10 compared with low resolution (mass resolution is defined as mass number divided by peak width, usually measured at 10% of its height).

Some instruments have provision for secondary-ion energy selection, which allows a degree of discrimination between monatomic and molecular ions by virtue of the difference between their energy distributions, a greater proportion of monatomic ions having higher energies. Shimizu *et al.* (1978), for example, found that by setting an energy threshold of 150 volts, errors (caused by molecular interferences) in *REE* isotope ratios in a silicate matrix could be greatly reduced. However, the use of isotope ratios as an indication of freedom from interferences has limitations: it is obviously not applicable to mono-isotopic *REE* such as Pr, Tb, Ho, or Tm, nor is it effective in cases such as La and Lu, which have only one major isotope.

Metson *et al.* (1983) have described a form of energy filtering whereby the specimen is allowed to 'float' electrically, reaching a negative potential of several hundred volts, which retards the secondary ions and allows only those with the highest energies to escape. Very effective suppression of molecular ions is obtained and the intensity loss is not prohibitive. However, a significant drawback of the 'specimen isolation' technique is that it is necessary to defocus the beam to about 50 μm, thereby sacrificing spatial resolution.

An alternative approach to the interference problem is 'spectrum stripping', as described, for example, by Colby (1975). Peak intensities (recorded at low resolution) are corrected by subtracting the contribution of interfering species, deduced from the intensity of isotopic variants of the same species. However, this procedure appears impracticable for *REE*, owing to the large number of possible interferences.

Interferences between REE. With isobaric interferences between *REE* (e.g. ^{150}Nd and ^{150}Sm) there is no possibility of resolving the peaks because the mass difference is very small. However, this is not an insurmountable problem, since every *REE* has at least one isotope that is free of such interferences (see fig. 1).

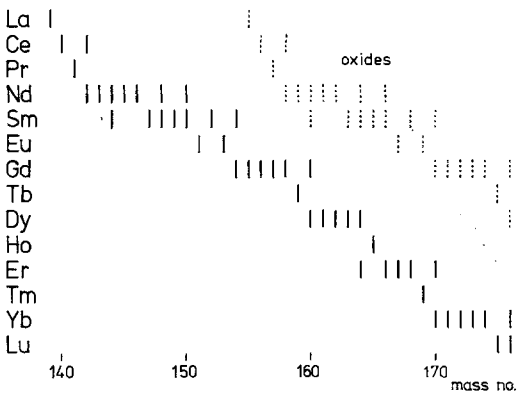

FIG. 1. The isotopes of the *REE* and their monoxides.

More seriously, light *REE* monoxides interfere with the atomic peaks of the heavy *REE*. Oxygen for oxide formation is abundant in most natural *REE* host phases and in any case is introduced by oxygen primary-ion bombardment. Furthermore, the *REE* are notable for their strong propensity for oxide secondary-ion formation. Consequently, *REE* oxide peaks are often more intense than the atomic peaks (figs. 3 to 7). The mass resolution of 8000 required to separate oxide and atomic peaks is not completely out of reach, but entails a prohibitive sacrifice in intensity.*

Further, energy discrimination is not very effective for *REE* oxides, because of the shape of the energy distribution. Measurements with a Cameca IMS-3f instrument showed that a twenty-fold intensity loss was incurred in obtaining a twenty times

* This statement is true for nearly all extant instruments; one exception is the instrument named 'SHRIMP' developed at the Australian National University (Compston *et al.*, 1982), which employs a large mass spectrometer capable of high transmission at such resolution.

reduction in the relative oxide intensity, the energy threshold used being 100 V (Reed, 1981). Conventional energy discrimination is thus a doubtful proposition in this case, though it should be noted that large *REE* oxide suppression factors have been obtained by the specimen isolation method mentioned above.

Oxide interferences from light *REE* thus appear to be unavoidable for *REE* heavier than Eu (see fig. 1). A possible strategy is to use the oxide peaks of the heavy *REE* for analytical purposes, thereby providing a means of determining *REE* from Dy upwards. For this to succeed it is necessary that the *dioxides* of the light *REE* should be insignificant, which fortunately appears to be so. Special difficulties are presented by Gd and Tb, inasmuch as their atomic peaks are subject to light *REE* oxide interference, while their own oxides lie within the mass range of the heavy *REE*. However, the oxide of ^{160}Gd (abundance 22%) coincides with ^{176}Lu, which has an abundance of only 2.6%, and in many cases can be neglected. The solitary Tb isotope (mass 159), on the other hand, has an oxide which coincides with the much more abundant ^{175}Lu and therefore is more likely to be affected.

Though *REE* monoxides are by far the most important interferences involving *REE* compounds, other possibilities exist. Hydroxides can be significant, especially when water is present in the sample, but are usually small by comparison with the oxides. A number of *REE* host phases contain F, causing fluoride interferences amongst the heavy *REE* similar to those caused by oxides, except for the different mass of F (19 rather than 16).

Matrix interferences. Apart from *REE* oxides, other molecules with masses in the *REE* region but composed entirely of matrix atoms also exist. Where the matrix contains only relatively light elements (up to Fe, say), molecules which interfere with *REE* peaks mostly contain at least four atoms. The number of possible combinations is large and molecular peaks generally appear at every mass number in the *REE* region. Fortunately these peaks are not usually very intense, but typically they correspond to *REE* concentrations in the range 1 to 50 ppm and can only be neglected when the *REE* peaks are much larger (*REE* concentrations in the hundreds of ppm range and upwards).

A possible test for the presence of interferences applicable to those *REE* which have two or more significant isotopes is to compare the observed isotopic peak intensities with the known natural isotope abundances (which are effectively constant in nearly all natural phases). Departure from the ideal relative abundances indicates the presence of interferences. For analytical purposes it is desirable to select the isotope least affected by interferences, i.e. the one giving the lowest value for the observed intensity divided by the natural abundance.

However, isotopic peaks chosen in this way are not necessarily entirely interference-free, and furthermore, half of the *REE* are mono-isotopic (or effectively so). The effect of matrix interferences can be eliminated by resorting to high mass resolution but this entails a considerable loss of intensity (e.g. a factor of ten or more, with most currently available instruments). Since the intensity falls rapidly with increasing resolution, the mass difference between a *REE* isotope and interfering molecule strongly influences the counting time required and the detection limits obtainable. An alternative method of suppressing interferences is energy discrimination, which is discussed in more detail later, but this also involves a considerable sacrifice in intensity. A final test for freedom from interferences which is peculiar to *REE* is the smoothness of the chondrite-normalized plot: as a working approximation it is reasonable to assume that *REE* concentrations (excluding Eu) expressed in this form should plot smoothly, any irregularity being a possible indication of undetected interferences. However, too much reliance should not be placed upon this assumption, since such irregularities may sometimes be genuine.

The mass difference between a *REE* isotope and an interfering matrix molecule (typically a small fraction of a mass unit) is governed by the mass of the atoms concerned. For example, in the spectrum of calcium phosphate there is a CaP_3O peak at mass 149, coinciding with an isotope of Sm. The mass defects of ^{40}Ca, ^{31}P, and ^{16}O are -37, -26, and -5 mmu respectively and the total mass defect of CaP_3O is therefore -120 mmu, compared with -83 mmu for ^{149}Sm. Thus the mass difference between the peaks is 37 mmu and the minimum resolution required to separate the peaks is $149 \div 0.037 \simeq 4000$.

While one can predict the resolution required in a particular case, there are so many possible molecular interferences in the *REE* region that it is impracticable to identify them all individually. However, the regularity of the relationship between mass defect and mass enables some general deductions to be made. In the region covering the common matrix elements ($m < 90$), the mass defects of all isotopes lie, with relatively little scatter, on a nearly straight line when plotted against mass. Molecules made up of such atoms therefore have mass defects also lying on straight lines (see fig. 2). The position of these lines depends on the number of atoms in the molecule, but is independent of the identity of the atoms, and hence of the matrix composition (unless heavy atoms are present in major amounts). The resolution of matrix molecule interferences can

therefore be considered in quite general terms (Reed, 1984).

It may be deduced from fig. 2 that mass resolution of about 4500 is necessary to separate a 4-atom molecule from ^{139}La; however, molecules of this type are increasingly easy to resolve with increasing *REE* mass. Molecules containing 5 atoms are less easily resolved, especially at the light end of the *REE* range, and this is even more so in the case of 6 atoms, but as a general rule, the larger the number of atoms, the smaller the molecular peak in the secondary-ion spectrum. It may be concluded that *REE* peaks can mostly be resolved from matrix interferences with a resolution of less than 5000, which is readily obtainable with current instruments.

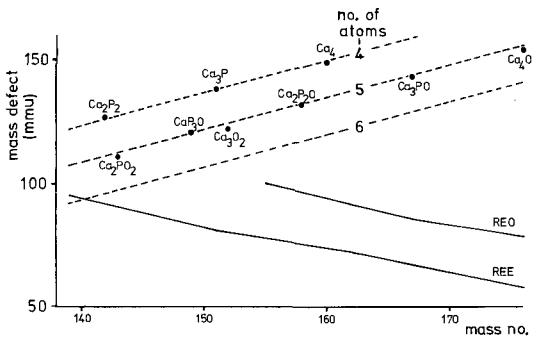

FIG. 2. The mass defects of molecular species occurring in the Ca phosphate spectrum compared to those of *REE* atoms and their monoxides, indicating the resolvability of the molecular interferences.

When heavy matrix elements are present, the interferences tend to be worse because the molecules concerned are simpler and the interfering peaks are more intense. For example, the mass spectrum of zircon contains numerous quite intense peaks in the *REE* region, arising from different combinations of Zr, Si, and O. However, these are reasonably resolvable, the resolution required being 2–4000 in most cases—*REE* determination in zircon is therefore not completely impracticable. Fortunately matrices with troublesome heavy elements are not common.

An element deserving special mention is Ba, which has isotopes in the mass range 130–138, with oxides between 146 and 154. These coincide with some of the isotopes of Sm, but can be avoided by using ^{147}Sm or ^{149}Sm, which are free from BaO interference. However, both of the Eu isotopes (151 and 153) are subject to such interference and the mass resolution required to separate the peaks is rather high (about 8000). Furthermore, energy discrimination is not very effective in this case. The presence of Ba therefore seriously impedes the determination of Eu.

Energy discrimination. Molecular ions containing several light atoms have narrow energy distributions, hence energy discrimination is quite effective in suppressing such interferences. For example, it has been observed that, while *REE* peak intensities are reduced by a factor of 50 with a threshold of 100 V, a molecular species such as Ca_2PO_3 (which interferes with Tb) is suppressed 10^4 times as much as the *REE* peaks (Crozaz and Zinner, 1985). In practice less discrimination would be sufficient in most cases and in general it should be possible to reduce matrix interferences to levels well below the equivalent of 1 ppm of *REE* quite easily, though still with considerable sacrifice in *REE* intensity.

It should be noted that the intensity sacrifice in the case of energy discrimination is an *inevitable* consequence of the overlapping energy distributions of molecular and atomic ions. In practice some loss of sensitivity also occurs at high mass resolution, but this is not absolutely unavoidable and indeed can be minimized by using a mass spectrometer of large dimensions. Energy filtering, however, is on the whole a more convenient method of suppressing matrix interferences, since its effectiveness is independent of mass difference, whereas the mass resolution required varies. Also measuring peak intensities at high mass resolution is more experimentally demanding.

Examples of REE spectra

Figs. 3 to 9 show secondary-ion spectra of a number of accessory minerals. The mass range of 139 to 192 includes all the significant atomic *REE* peaks and their monoxides. Peak intensities are in counts/s on a logarithmic scale. These spectra show various features relevant to *REE* determination.

The *REE* phosphate *monazite* has a high total *REE* content, with depleted heavy relative to light *REE*. In the example shown in fig. 3 the strong downward trend in concentrations is reflected both in the atomic peaks from 139 to 155 (La–Eu) and the oxide peaks from 156 to 192. The oxide peaks are more intense than the corresponding atomic peaks, e.g. CeO (156) is about six times more intense than Ce (140). This is typical of *REE* spectra, and with the marked downward concentration trend in this case, ensures that where *LREE* oxide and *HREE* atomic peaks are both present (from 156 to 176) the former are dominant.

Fig. 4 shows a typical spectrum of *sphene* ($CaTiSiO_5$), a fairly common *REE* host phase. This spectrum is similar to that of monazite, but with lower intensities overall, owing to the lower *REE*

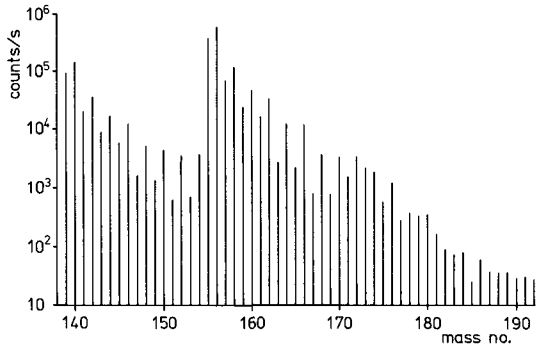

FIG. 3. Secondary-ion mass spectrum of monazite, covering all significant *REE* and monoxide peaks, from La (139) to LuO (192). Peaks can be identified by reference to fig. 1. Monoxide peaks are dominant above mass 155 (LaO), the *HREE* atomic peaks being comparatively insignificant, owing to the relatively low concentrations of *HREE* in this phase.

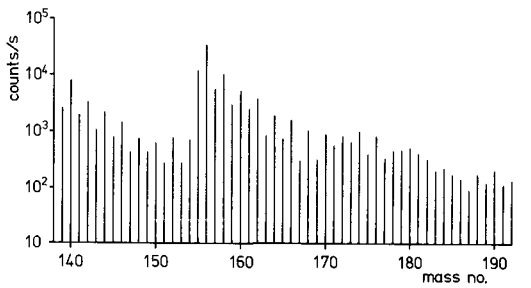

FIG. 4. Spectrum of sphene, with flatter *REE* distribution than monazite (fig. 3), but exhibiting similarly prominent *LREE* oxide peaks.

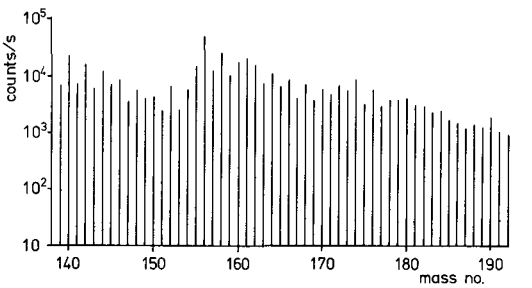

FIG. 5. Spectrum of spencite, a borosilicate with a fairly flat *REE* distribution, showing more intense *HREE* oxide peaks than the previous examples (figs. 3 and 4).

concentrations (e.g. about 1% Ce). The fractionation in favour of *LREE* is less marked in the case of sphene.

The spectrum in fig. 5 is that of *spencite*, a borosilicate mineral with *REE* concentrations around the 1% level. The *REE* peak intensities show a moderate decrease with increasing mass, which reflects a decrease in ion yield rather than in concentration (see next section). Spencite has a high water content (11%), giving rise to significant hydroxide peaks which add an extra complication to the interpretation of the spectrum (Reed, 1984).

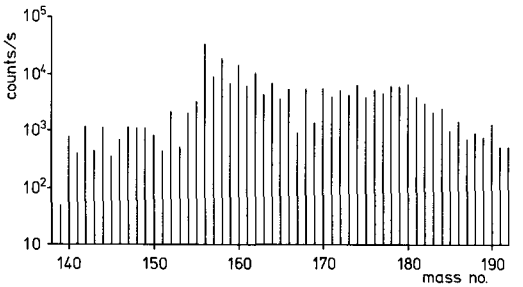

FIG. 6. Uraninite spectrum: in this case the *HREE* are enriched relative to the *LREE* (note the very small La peak at mass 139).

The *uraninite* spectrum in fig. 6 shows exceptionally intense oxide peaks, e.g. the CeO/Ce ratio is about 50. This may be attributable to the presence of excess oxygen arising from the decay of U^{4+} to Pb^{2+}.

The high concentration of F in *fluocerite* (a natural *REE* fluoride) results in intense fluoride peaks in the mass spectrum. In fig. 7 the LaF and CeF peaks at masses 158 and 159 are of comparable intensity to the corresponding oxides at 155 and 156 (the only source of oxygen for the formation of

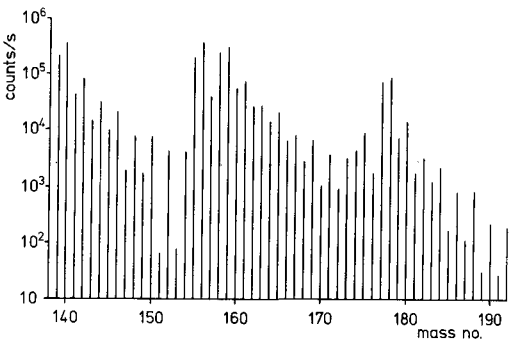

FIG. 7. Spectrum of fluocerite (a *REE* fluoride phase), showing strong fluoride and difluoride peaks (e.g. LaF at 158 and LaF_2 at 177) as well as the usual oxide peaks (in this case derived entirely from the primary ion beam oxygen). Also notable is the marked Eu depletion evidenced by the low intensity of the 151 and 153 peaks.

oxides in this case is that introduced by primary beam implantation and the ratio of *REE* oxide to atomic peaks is lower than for oxygen-containing phases). Difluorides can also be seen at 177 (LaF_2) and 178 (CeF_2) in contrast to the almost complete absence of *REE* dioxides. The anomalously small peaks at 151 and 153 are those of Eu, which is evidently depleted in this phase.

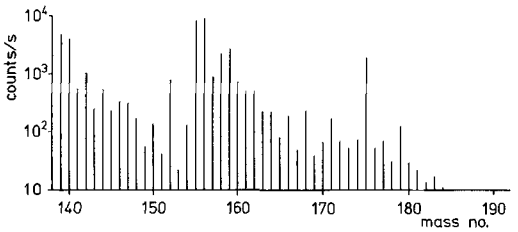

FIG. 8. Fluorapatite spectrum, with visible but much smaller fluoride peaks than fluocerite (fig. 7), and relatively low *REE* concentrations (e.g. Ce 0.37%, Yb 27 ppm).

Smaller fluoride peaks are also visible in the *fluorapatite* spectrum (fig. 8), the concentration of F being considerably lower in this case (about 4%). The *REE* concentrations are relatively low, being around 0.1% for *LREE*, falling to less than 10 ppm for Lu. With smaller peaks, matrix interferences become more significant (obvious interferences can be seen at 152 and 175).

A spectrum of unusual appearance is observed in the case of *xenotime* (YPO_4), as shown in fig. 9. This phase has a strong preference for heavy *REE*, these being present in concentrations of the order of 1%. The *REE* abundances fall off very steeply at the light end (the concentration of La is only about 5 ppm). The *LREE* oxides are not visible because they are insignificant by comparison with the atomic peaks of the much more abundant *HREE* occurring at the same masses.

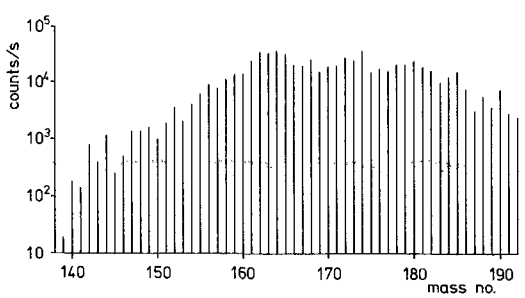

FIG. 9. Spectrum of xenotime, which has a marked preference for *HREE*, with *LREE* concentrations falling to about 5 ppm for La. In this case the *LREE* oxides are not visible amongst the atomic *HREE* peaks.

Quantification

Having measured the intensities of the *REE* peaks (either avoiding, or correcting for, interferences) it remains to translate these into concentrations. This requires a knowledge of the relevant secondary-ion yields. In case of *REE*, the problem can be treated in two parts—first the determination of *relative REE* concentrations (as required for plotting abundance patterns), and secondly the conversion of these into *absolute* concentrations. For the latter purpose it is necessary to measure the intensity of some suitable internal standard peak (e.g. Ca, Si, etc.) together with the *REE* peaks. For calculating *REE* concentrations, the ion yield of the reference element relative to the *REE* must then be known. The determination of relative *REE* concentrations merely requires information on the variation in ion yield amongst the *REE*.

Secondary-ion production is a complex and incompletely understood phenomenon. Some success in predicting ion yields has been achieved with the local thermal equilibrium model of Andersen and Hinthorne (1973), but this model is not applicable to *REE*, the anomalous behaviour of which is probably related to their strong tendency to form oxides. In the absence of a theoretical procedure for predicting ion yields in this case, quantification of analytical results is dependent on empirical data.

The *REE*-containing silicate glass standards produced by Drake and Weill (1972) are especially useful because each of the four otherwise identical standards contains only three or four *REE*, thereby avoiding oxide interferences. Fig. 10 shows the relative yields of atomic *REE* ions derived from these standards (note that both atomic and oxide intensities are normalized to La = 1 in this diagram—in most cases the actual intensity of the oxides is greater). Contrary to initial expectations, these quite widely varying yields are not related to the ionization potential (Reed, 1983). It seems that oxide ion formation has a dominant effect on atomic *REE* ion formation, and comparison with the oxide ion yields also shown in fig. 10 reveals a fairly close anti-correlation, consistent with competition between oxide and atomic ion formation. *REE* spectra show a wide range of relative oxide intensities (see previous section), and obviously this must be taken into account in any scheme for quantitative analysis.

The ratio of oxide to atomic peak intensity, MO^+/M^+, is quite closely correlated with oxide bond energy (Ishizuka, 1974), or more rigorously

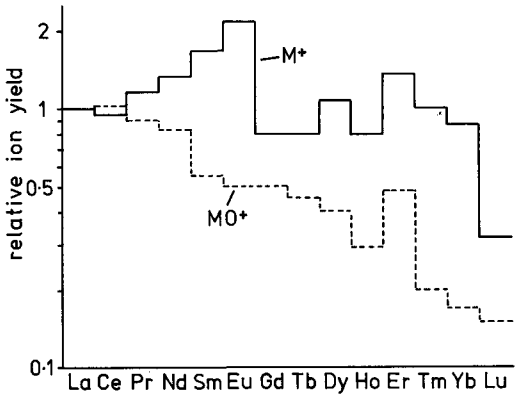

FIG. 10. Yields of atomic and monoxide secondary ions, both normalized to unity for La, obtained from silicate glass standards (Reed, 1983), showing widely varying yields amongst the *REE*, with negative correlation between atomic and oxide ion yields for *LREE* and more complex behaviour of *HREE*.

with the modified bond energy, E'_{MO}, which takes account of the difference in ionization potential between atom and oxide (Reed, 1983). Fig. 11 shows a logarithmic plot of MO^+/M^+ against E'_{MO} for the Drake and Weill silicate glasses. Except for Lu, which behaves anomalously, the points lie fairly close to a straight line, as expected for a thermally activated process.

In the case of natural phases containing all 14 *REE*, it is possible to determine MO^+/M^+ for the *LREE* (La-Eu), provided that the *HREE* atomic peaks occurring at the same masses as the *LREE* oxides are small enough to be neglected (or corrected for). However, it is usually difficult, if not impossible, to measure both the oxide and atomic peaks of the *HREE* (Gd-Lu), hence we do not have complete sets of MO^+/M^+ values for different natural phases. However, as shown in fig. 11, plots of *LREE* data lie on straight lines, which can

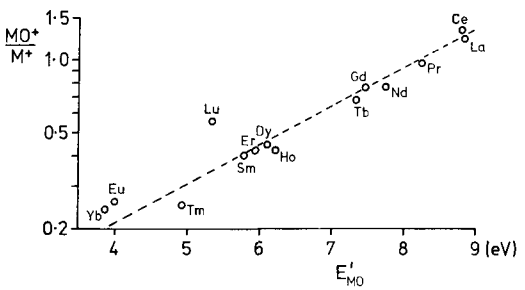

FIG. 11. Ratio of oxide to atomic ion yields for *REE*, plotted against effective bond energy E'_{MO} (Reed, 1983).

reasonably be extrapolated to obtain estimated values for the *HREE*.

If elemental *REE* ion yields could be predicted, it would thus also be possible to derive oxide ion yields when required. The data from the Drake and Weill glasses, while giving a useful indication of elemental yield variations, are not necessarily applicable to other matrices. In the absence of a valid theoretical model, we do not yet know how to take account of the effect of matrix composition on *REE* ion yields.

Presumably the readily observable differences in oxide/element peak intensity ratios are indicative of differences in ionization conditions. High oxide/element ratios may be a consequence of high oxygen concentration, either inherent in the sample composition or resulting from primary implantation (the implanted concentration being a function of sputtering rate). However, it is possible that other parameters also influence oxide ion formation. The simplest assumption as regards the effect of *REE* oxide formation in the secondary ion spectrum is that oxide and elemental ion production are competing processes and therefore give yields that are negatively correlated. However, it is known that oxygen, having a high affinity for electrons, has the general effect of enhancing positive ion production, and this enhancement will presumably vary with the effective oxygen concentration. Further, this effect may to some extent act differentially as between *REE* (depending perhaps on ionization potential). At present there is insufficient evidence from measurements on *REE* of known concentration in different matrices to enable a generalized method of matrix correction to be formulated, taking the various possible effects into account.

Examples of applications

Allanite. The epidote-group mineral allanite, essentially a Ca-Fe aluminosilicate with a total *REE* oxide content in the vicinity of 25-30%, is an important *REE* phase in many granitic and related rocks, as well as in pegmatites. Its *REE* distribution characteristically shows a steep downward trend, with concentrations ranging from about 10% Ce to 10 ppm Lu. Half of the *REE* are near or below the detection limit for electron microprobe analysis, which can therefore provide information neither on the form of the distribution at the heavy end, nor the extent of the Eu depletion. With the ion microprobe, however, all the *REE* are detectable in the allanite spectrum (fig. 12), though for some of the *HREE* peaks, interferences are quite significant. For example a large molecular peak interferes with $^{169}Tm^{16}O$, and cannot be avoided by choice of alternative isotope, as is sometimes the case, because

Tm is mono-isotopic. With a mass difference of about 45 mmu, this interference is resolvable—the minimum resolution needed being about 4000—but only with considerable intensity loss. Though energy discrimination would presumably be effective, a considerable intensity loss would also be entailed.

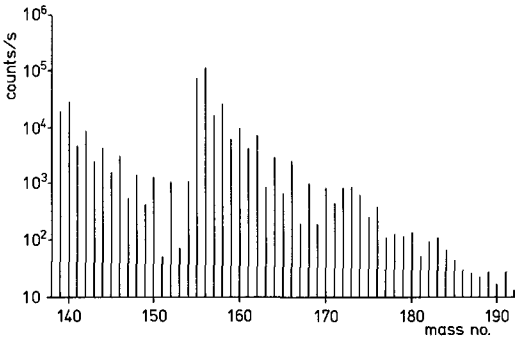

FIG. 12. Secondary-ion spectrum of *REE* in typical allanite (Amitsoq gneiss): note dominance of oxide peaks above mass 155.

For the purpose of absolute quantitative analysis it is necessary to compare the *REE* peak intensities with a major element of known concentration. For allanite the best choice is probably Ca, though its concentration varies significantly and must be determined (e.g. by electron microprobe analysis) in each case. The ^{40}Ca peak, however, is excessively intense and may overload the counting system, hence it is better to use ^{44}Ca (2% abundance). Owing to differences in the energy distributions of Ca and *REE* ions, instrument-dependent discrimination effects influence the repeatability of *REE*/Ca ratios (Reed, 1985). This, among other things, limits the absolute accuracy with which *REE* can be determined, and since some of the light *REE* are present in concentrations of several percent, it is preferable to rely on the electron microprobe for determining these absolutely, using ion microprobe data for Eu and *HREE* to complete the distribution pattern.

Since matrix effects in ion-probe analysis are poorly understood, it is desirable to use an analysed allanite as the standard for determining *REE* in other allanites. An example of a suitable candidate is the allanite from Sandy Braes obsidian (N. Ireland), described and analysed by Brooks *et al.* (1981). The analysis in Table II is incomplete as regards *REE*, hence some *REE* concentrations must be obtained by chondrite-normalized interpolation. Fig. 13 shows the results of ion-probe analysis of another allanite, using Sandy Braes as the standard. Interference corrections (which may vary somewhat between different allanites, with varying proportions of Ca, Al, Si, Fe, and minor elements) were determined using high mass resolution. In fig. 13 the Ce concentration is normalized to the electron microprobe value, as suggested above.

TABLE II. *Composition of Sandy Braes allanite (after Brooks* et al., *1981)*

	wt. %		ppm
SiO_2	31.2	Eu	110
Al_2O_3	14.3	Gd	2600*
CaO	10.1	Tb	200
FeO	15.5	Dy	840*
La	4.9	Ho	120*
Ce	10.5	Er	220*
Pr	1.1*	Tm	22*
Nd	3.5	Yb	90
Sm	0.41	Lu	10

* Estimated by interpolation on chondrite-normalized basis.

Apatite. This is an example of a phase which may contain minor but significant concentrations of *REE*, which are, however, near or below the detection limit of electron microprobe analysis in most cases. Interferences from molecules containing Ca, P, and O occur throughout the *REE* region but can nearly always be resolved, as discussed earlier (see fig. 2), or suppressed by energy discrimination. The interferences are somewhat influenced by whether the apatite is of the fluor-, chlor-, or hydroxy- variety (in the case of fluorapatite *REE* fluoride peaks are significant—see fig. 8).

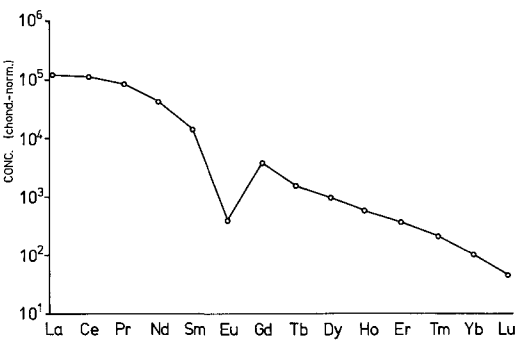

FIG. 13. *REE* in allanite, plotted in chondrite-normalized form, as determined with the ion probe (Reed, 1985).

TABLE III. *REE concentrations and ion yields for Durango apatite*

Element	Isotope used	Concentration (ppm)	Intensity (relative to La)	Ion yield (relative to La)
La	139	3000	1.00	1.00
Ce	140	3700	0.73	0.66
Pr	141	300†	0.098	0.98
Nd	146	1000	0.065	1.09
Sm	149	135	0.0090	1.43
Eu	151	17	0.0070	2.60
Gd	174*	100†	0.0089	1.02
Tb	175*	16	0.0048	0.87
Dy	180*	90†	0.0045	0.52
Ho	181*	17†	0.0030	0.51
Er	182*	40†	0.0021	0.40
Tm	185*	5	0.00070	0.41
Yb	190*	27	0.00080	0.28
Lu	191*	3	0.00030	0.28

* Oxide.
† Estimated by interpolation on chondrite-normalized basis.

An apatite useful as a standard is that from Durango, Mexico (Young *et al.*, 1969), which has unusually high *REE* concentrations (e.g. 0.37% Ce), though with a marked downward trend from light to heavy *REE*. As in the case of allanite, only incomplete *REE* data are available and the remaining concentrations have to be estimated by interpolation on a chondrite-normalized basis (see Table III).

For the determination of *REE* in phases such as apatite, the ion microprobe is quicker and more convenient than procedures currently used which involve mineral separation prior to analysis by a bulk method such as NAA. In the case of scarce extra-terrestrial material such as meteorites and lunar samples, the near non-destructiveness of the ion microprobe is an additional benefit. Recent studies of *REE* in phosphate phases in chondritic meteorites are a case in point. In chondrites, the Ca-phosphate merrillite (closely related to whitlockite) coexists with apatite (mostly of the chlor- variety) and has been shown to have *REE* concentrations about five times higher (see fig. 14). This partitioning behaviour is relevant to studies of Pu chronology, and tends to support the assumption sometimes made, that Pu and *REE* behave similarly (Reed and Smith, 1983, 1985; Crozaz and Zinner, 1985). Another interesting aspect of the ion microprobe results is the determination of the negative Eu anomaly in chondritic phosphates and its relation to their thermal history.

Also, *REE* determination in merrillite (as the principal host phase) throws light on bulk chondritic *REE* distribution patterns. Bulk chondrite analyses mostly show fairly consistent patterns, which are the basis for the 'solar system' values used for normalization. However, quite large anomalies have sometimes been reported, suggesting heterogeneity in primitive planet-forming material. Though not conclusively disproving the existence of these anomalies, ion microprobe analyses of merrillite in chondrites have so far failed to confirm their existence (Reed and Smith, 1985).

In passing, it may be noted that no significant matrix effects have been found, as between fluorapatite, chlorapatite, and merrillite (which has somewhat different proportions of Ca and P, and

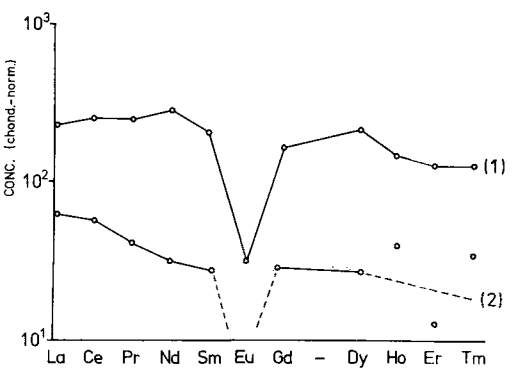

FIG. 14. *REE* in the phosphates merrillite (1) and apatite (2) in the Salles meteorite, determined with the ion probe (Reed and Smith, 1983). Note: Tb, Yb, Lu in both phases, and Eu in apatite, not determined; *HREE* in apatite not corrected for interferences.

contains Na and Mg at the few percent level). Evidence on merrillite was obtained from lunar material with *REE* concentrations high enough for electron microprobe determination.

Ion microprobe analysis of apatite in chondrites is hampered by the generally small size of the grains and the low *REE* concentrations (mostly below fifty times bulk chondritic values). Some lunar rocks have phosphates with higher *REE* concentrations, which have been determined by electron microprobe analysis. However, the ion microprobe has also been used to analyse lunar phosphates, including apatite with *REE* predominantly near or below the electron microprobe detection limit (Lindstrom *et al.*, 1985).

A further recent application is to apatite in a phosphate-rich clast in the 'lunar meteorite' ALHA 81005 (a meteorite of lunar origin, found in Antarctica). Here the amount of material available is very small and exists only in thin section, precluding the use of bulk analysis methods. The *REE* in whitlockite in this material are within the range of the electron microprobe, but not in the co-existing apatite. As shown in fig. 15, the ion microprobe data indicate *REE* concentrations of around 200 times bulk chondritic values in the apatite, with a fairly flat chondrite-normalized distribution pattern (apart from the negative Eu anomaly).

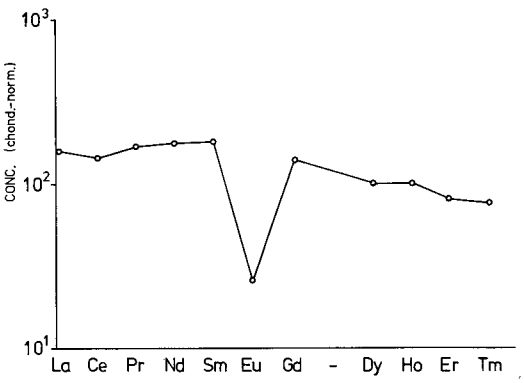

FIG. 15. *REE* in apatite in lunar meteorite ALHA 81005, as determined with the ion probe (Goodrich *et al.*, 1985).

In cases where *REE* concentrations are in the ppm region, with significant interferences, secondary-ion collection efficiency is critical, in so far as the interferences demand the use of either high mass resolution or energy discrimination, both of which reduce the already low peak intensities. In this situation the high transmission obtainable at high resolution with an instrument such as 'SHRIMP' (Compston *et al.*, 1982) is especially valuable. In order to investigate the potential of this instrument, measurements were made on a synthetic apatite (BM 1919, 333) with quite low *REE* content, at a mass resolution of 8000 (presumed to be sufficient to resolve most interferences attributable to matrix molecules). At this resolution, the ^{139}La intensity with a primary beam current of 8 nA was 35 counts/s per ppm, so that *REE* peaks at ppm levels could easily be measured.

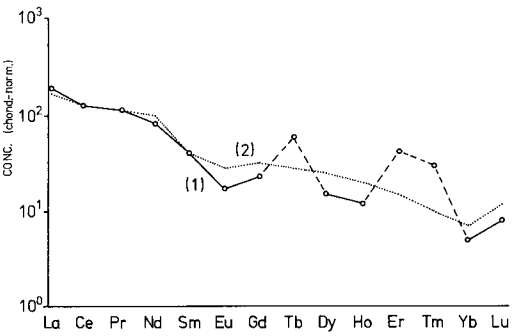

FIG. 16. Chondrite-normalized concentrations of *REE* in apatite (BM 1919, 333), as determined by ion probe (1) and INAA (2). Ion-probe data obtained at mass resolution of 8000, thereby avoiding most interferences (apart from Tb, Er, and Tm, which give high values, presumably owing to incompletely resolved interferences).

REE concentrations for the low-*REE* apatite, using Durango apatite as standard, are plotted in fig. 16, together with INAA data for the same material. The chondrite-normalized plot is reasonably smooth and agreement with the INAA data is fairly satisfactory, except for Tb, Er, and Tm, for which the ion probe gives values which are apparently too high, probably because of unresolved interferences. In terms of absolute concentration, the largest error is 6 ppm (for Er).

Sphene ($CaTiSiO_5$) is a common accessory mineral in igneous rocks and can accommodate *REE* at concentrations varying up to the percent level. The examples given here are from a granitoid series occuring at McMurry Meadows, Sierra Nevada (Sawka *et al.*, 1984). The *REE* concentrations in sphene are relatively high in the granitic core of the pluton and decrease towards the edge (quartz monzodiorite). The shape of the chondrite-normalized distribution also changes somewhat (see fig. 16), the most obvious difference being the change from a negative to a positive Eu anomaly.

Electron-probe data for La, Ce, Nd, Dy, and Yb in one of the high-*REE* sphene samples were used

as the basis for the ion-probe determinations represented in fig. 17. Interferences were found to be negligible in the granitic sphenes, with *REE* concentrations ranging from 10^3 times chondritic upwards, and significant but not serious for *HREE* in quartz monzodiorite sphenes (around 10^2 times chondritic). Ion-probe determination of complete *REE* distributions is therefore quite straightforward.

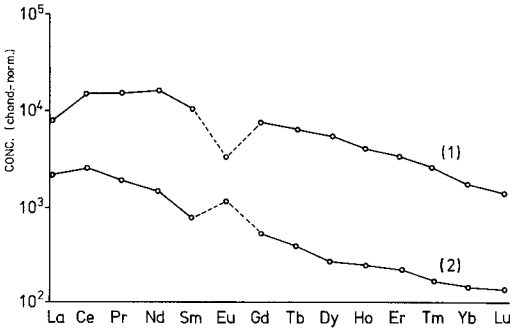

FIG. 17. *REE* in sphenes (McMurry Meadows granodiorite complex) determined with the ion probe: (1) granite, (2) quartz monzodiorite.

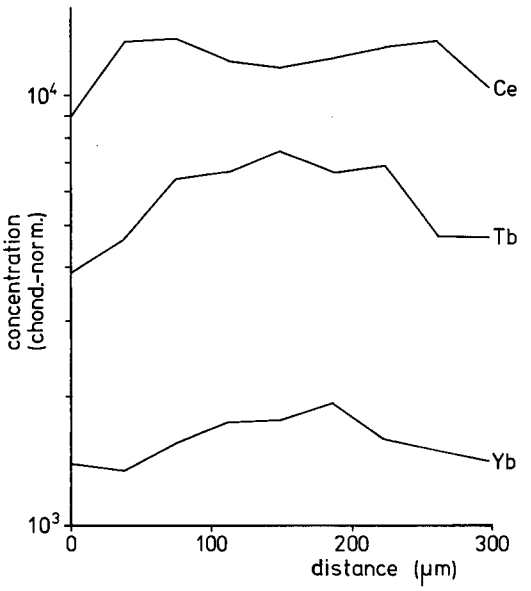

FIG. 18. Distribution of Ce, Tb, and Yb across sphene grain in granite (McMurry Meadows granodiorite complex), showing differences in profiles of *LREE* and *HREE*.

REE zoning in these sphenes, as revealed by the electron microprobe, has been discussed by Sawka *et al.* (1984). Ion-probe profiles for Ce, Tb, and Yb across a zoned granitic sphene grain show differential zoning effects (fig. 18).

Chevkinite. The relatively uncommon accessory mineral is an Fe-Ti silicate with a high *REE* content and typically contains minor amounts of Ca, Mn, Zr, Nb, and Th. In a chevkinite from E. Greenland (supplied by M. Brown), the *LREE* were determined by energy-dispersive electron-probe analysis, with the following results (in wt. %): La_2O_3 12.7, Ce_2O_3 23.1, Pr_2O_3 2.0, Nd_2O_3 6.5. The other *REE*, being below the limit for reliable estimation by this technique, were determined with the ion probe. The electron probe data for La–Nd were combined with the ion-probe results for the rest of the *REE* to give the chondrite-normalized plot shown in fig. 19. Interferences being small in this case, the measurements were made at low mass resolution. In the absence of an analysed chevkinite standard, the Sandy Braes allanite (see above) was used.

The oxide/element peak intensity ratios in the chevkinite spectrum are two to three times higher than for allanite. In order to allow for this, the following procedure was adopted. First, the *HREE* oxide peak intensities obtained from the allanite were converted to elemental ion yields with the aid of a plot of oxide/element ratio against E'_{MO} (as in fig. 11), based on measurements on the *LREE* peaks and their oxides. It was assumed that the atomic yields were the same in chevkinite, and they were converted into the required *HREE* oxide yields by means of a similar plot using the measured *LREE* oxide/element ratios for chevkinite. Though somewhat arbitrary, this approach should at least approximately take account of the difference in the propensity for oxide ion formation in the two phases concerned. The data plotted in fig. 19 were normalized so as to agree with the electron-probe value for Ce, thereby eliminating any dependence on knowledge of the absolute *REE* ion yields.

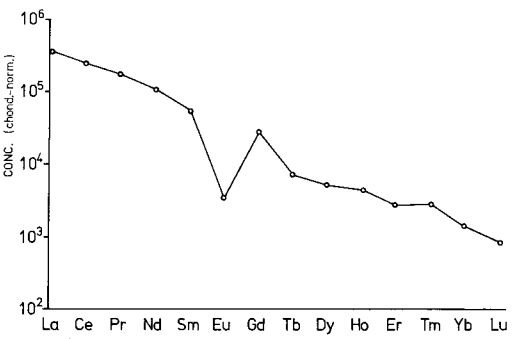

FIG. 19. Chondrite-normalized concentrations of *REE* in chevkinite, obtained by combining electron-probe results for La–Nd with ion-probe data for Sm–Lu.

Conclusions

The ion microprobe has a variety of actual and potential applications in earth sciences and one which seems particularly promising is *REE* determination in accessory minerals. Much lower detection limits are attainable than with the electron microprobe, and compared with techniques such as INAA, currently used for trace *REE* analysis, specimen preparation is very simple and physical mineral separation is unnecessary.

Mass interferences in the secondary-ion spectrum are a nuisance but do not present an insuperable problem: *LREE* oxides can be avoided by using the oxide peaks of the *HREE* for analytical purposes, while matrix molecules can either be suppressed by energy discrimination or else the interfering peaks can be resolved, the mass resolution required usually being less than 5000.

Quantification presents difficulties in view of the lack of a viable theoretical model of the secondary ionization process applicable to the *REE*. At present, quantitative analysis is therefore largely dependent on analysed standards, which preferably should be close to the 'unknown' in composition. However, if only relative *REE* concentrations are required, the problem is less severe, since relative *REE* ion yields appear to be more predictable, the main determinant being the varying propensity for oxide ion formation in different matrices.

The instrument used to obtain the results presented here has inherent limitations as regards secondary-ion collection efficiency. New-generation ion microprobe instruments will give considerably higher count-rates, enabling lower concentrations of *REE* to be detected (e.g. below the 1 ppm level), thereby opening up further areas of application, e.g. to rock-forming phases, including silicates. Other anticipated benefits include improvement in spatial resolution to maybe about 1 μm, made possible by the lower primary beam current required to produce a given secondary-ion intensity.

Acknowledgements. I am indebted to the following for loans and donations of samples: M. Brown, University of Aberdeen (chevkinite); N. R. Charnley, University of Oxford (spencite); A. M. Clark, British Museum (Natural History) (apatite); R. A. Exley, University of Chicago (allanite); L. Kanat, University of Cambridge (xenotime); D. G. W. Smith, University of Alberta (apatite, monazite); M. Styles, British Geological Survey (fluocerite); W. N. Sawka, Australian National University (sphene). Thanks are also due to W. Compston and I. S. Williams of the Australian National University for making possible the use of the 'SHRIMP' instrument. The invaluable contribution of colleagues in the Cambridge Ion Probe Laboratory, especially J. V. P. Long and R. A. Mason, and financial support from the Natural Environment Research Council, are gratefully acknowledged.

REFERENCES

Andersen, C. A., and Hinthorne, J. R. (1973) *Anal. Chem.* **45,** 1421–38.

Banner, A. E., and Stimpson, B. P. (1974) *Vacuum,* **24,** 511–17.

Brooks, C. K., Henderson, P., and Rønsbo, J. G. (1981) *Mineral. Mag.* **44,** 157–60.

Colby, J. W. (1975) In *Practical Scanning Electron Microscopy* (J. I. Goldstein and H. Yakowitz, eds.), Plenum, New York, 529–72.

Compston, W., Williams, I. S., and Clement, S. W. (1982) In *Proc. 30th Ann. Conf. on Mass Spectrometry and Allied Topics,* Honolulu, Am. Soc. Mass Spectrom., 592–5.

Crozaz, G., and Zinner, E. (1985) *Earth Planet. Sci Lett.* **73,** 41–52.

Degreve, F., Figaret, R., and Laty, P. (1979) *Int. J. Mass Spectrom. Ion Phys.* **29,** 351–61.

Drake, M. J., and Weill, D. F. (1972) *Chem. Geol.* **10,** 179–81.

Goodrich, C. A., Taylor, G. J., Keil, K., and Reed, S. J. B. (1985) In *16th Lunar and Planetary Sci. Conf. Abstr.,* 282–3.

Haskin, L. A., Haskin, M. A., Frey, F. A., and Wildeman, T. R. (1968) In *Origin and Distribution of the Elements* (L. H. Ahrens, ed.), Pergamon, New York, 869–912.

Henderson, P. (1984) *Rare Earth Element Geochemistry.* Elsevier, Amsterdam.

Ishizuka, T. (1974) *Anal. Chem.* **46,** 1487–91.

Lindstrom, M. M., Crozaz, G., and Zinner, E. (1985) *Lunar Planet. Sci.* **16,** 493–4.

Long, J. V. P., Astill, D. M., Coles, J. N., Reed, S. J. B., and Charnley, N. R. (1980) In *X-ray Optics and Microanalysis* (D. R. Beaman, R. E. Ogilvie, and D. B. Wittry, eds.), Pendell Publ. Corp., Midland, Mich., 316–21.

Metson, J. B., Bancroft, G. M., McIntyre, N. S., and Chauvin, W. J. (1983) *Surf. Interf. Anal.* **5,** 181–5.

Reed, S. J. B. (1981) In *Microbeam Analysis—1981* (R. H. Geiss, ed.), San Francisco Press, San Francisco, Calif., 87–90.

——(1983) *Int. J. Mass Spectrom. Ion Processes,* **54,** 31–40.

——(1984) *Scanning Electron Microscopy 1984,* 529–35.

——(1985) *Chem. Geol.* **48,** 137–43.

—— and Smith, D. G. W. (1983) *Nature,* **306,** 172–3.

—— ——(1985) *Earth Planet. Sci. Lett.* **72,** 238–44.

Sawka, W. N., Chappell, B. W., and Norrish, K. (1984) *Geology,* **12,** 131–4.

Shimizu, N., Semet, M. P., and Allegre, C. J. (1978) *Geochim. Cosmochim. Acta,* **42,** 1321–34.

Young, E. J., Myers, A. T., Munson, E. L., and Conklin, N. M. (1969) *U.S. Geol. Surv. Prof. paper* 650D, 84–93.

[*Manuscript received 12 July 1985; revised 2 October 1985*]